Non-linear Shear and Uniaxial Extensional Rheology of Polyether-Ester-Sulfonate Copolymer Ionomer Melts

Shabbir, Aamir; Huang, Qian; P. Baeza, Guilhem ; Vlassopoulos, Dimitris; Chen, Quan; H. Colby, Ralph ; J. Alvarez, Nicolas; Hassager, Ole

Published in:
Journal of Rheology

Link to article, DOI:
10.1122/1.4998158

Publication date:
2017

Document Version
Publisher's PDF, also known as Version of record

Nonlinear shear and uniaxial extensional rheology of polyether-ester-sulfonate copolymer ionomer melts

Aamir Shabbir, Qian Huang, Guilhem P. Baeza, Dimitris Vlassopoulos, Quan Chen, Ralph H. Colby, Nicolas J. Alvarez, and Ole Hassager

Citation: Journal of Rheology **61**, 1279 (2017);
View online: https://doi.org/10.1122/1.4998158
View Table of Contents: http://sor.scitation.org/toc/jor/61/6
Published by the The Society of Rheology

Nonlinear shear and uniaxial extensional rheology of polyether-ester-sulfonate copolymer ionomer melts

Aamir Shabbir and Qian Huang

Department of Chemical and Biochemical Engineering, Technical University of Denmark, Kongens Lyngby 2800, Denmark

Guilhem P. Baeza and Dimitris Vlassopoulos

Institute of Electronic Structure and Laser, FORTH, Heraklion 71110, Crete, Greece, and Department of Materials Science and Technology, University of Crete, Heraklion 71003, Crete, Greece

Quan Chen and Ralph H. Colby

Department of Material Science and Engineering, Pennsylvania State University, University Park, Pennsylvania 16802

Nicolas J. Alvarez

Department of Chemical and Biological Engineering, Drexel University, Philadelphia, Pennsylvania 19104

Ole Hassager[a)]

Department of Chemical and Biochemical Engineering, Technical University of Denmark, Kongens Lyngby 2800, Denmark

(Received 12 September 2016; final revision received 26 July 2017; published 1 November 2017)

Abstract

We present unique nonlinear shear and extensional rheology data of unentangled amorphous polyester ionomers based on polyethers and sulphonated phthalates with sodium/lithium counterions. Previous linear viscoelastic measurements showed significant elasticity in these ionomers due to the formation of strong ionic aggregates. These ionomer melts exhibit viscoelastic properties similar to well-entangled melts with an extended rubbery plateau. To evaluate the effects of nonlinear deformation, the rheology of these ionomers was investigated using uniaxial extension and shear. The measurements were performed on a filament stretching rheometer and on a strain controlled rotational rheometer equipped with a cone-partitioned-plate setup. In extension, ionomer samples exhibited a decreasing strain hardening trend with increasing extension rates. At the same Weissenberg number, the same strain hardening was observed for different counterions. The presence of high solvating poly(ethylene oxide), PEO, along the backbone in the coionomer with poly(tetramethylene glycol), PTMO, increases the maximum Hencky strain at fracture, thus adding ductility to the brittle PTMO-Na ionomer. As a result, the coionomer deforms much more compared to PTMO-Na, but eventually, both fracture. On the other hand, whereas PTMO-Na cannot be sheared due to wall slip, the coionomer deforms in shear and eventually suffers from edge fracture instabilities. From the above, a picture emerges suggesting that PEO coionomers enhance ductility, make fracture smoother and offer a compromise of mechanical performance and ion conduction. © *2017 The Society of Rheology*. [http://dx.doi.org/10.1122/1.4998158]

I. INTRODUCTION

Ionomers represent a family of polymers where ionic groups are covalently attached to the polymer backbone. Due to the strong dipolar interaction between the ion pairs, ionic groups have a tendency to bond into nanometer-sized aggregates (which can nanophase separate into ionic clusters) within the polymer matrix, and thus, act as temporary crosslinks [1]. Viscosity and elasticity of ionomer melts are typically several orders of magnitude higher compared to their nonionic counterparts because of retarded diffusional motion of polymer chains. The ion pairs attached to the polymer chains relax by a mechanism, which involves many jumps from one cluster to another, often termed as "ionic hopping" [2], before the whole chain can relax completely [1,3].

The linear rheology of ionomer melts has been studied quite extensively by many research groups [1,3–8]. In contrast, little is known about the nonlinear viscoelasticity of ionomers, in particular under extensional flows. Connelly *et al.* [9] were the first to study extensional properties of

[a)]Author to whom correspondence should be addressed; electronic mail: oh@kt.dtu.dk

ionomers in 1982. Takahashi *et al.* [10] investigated the effects of ionic interaction on the uniaxial extensional flow of ethylene-based ionomer melts. Stadler *et al.* [11] studied the extensional behavior of entangled telechelic polybutadiene (PBd) carboxylate ionomers and reported on the dependence of strain hardening on various counterions (Rb, Na, K, and Li). The authors qualitatively discussed the influence of cohesive strength of ionic clusters on the strain hardening behavior. Weak ionic clusters (largest, Rb) exhibit fluidlike behavior, medium strength clusters (K) exhibit noticeable strain hardening, and strong ionic clusters (Na, Li) are too brittle to study strain hardening [11]. More recently, Weiss and coworkers [12] studied extensional rheology of nearly monodisperse alkali metal neutralized oligomeric sulfonated polystyrene ionomers. The effect of ionic associations was isolated since the systems studied were below the entanglement molecular weight of polystyrene. They reported strain hardening for extension rates greater than the inverse of sticker lifetime and concluded that a maximum in engineering stress under extensional deformation resulted from the catastrophic failure of the transient network and was nearly independent of extension rate. Ionomers have been shown to exhibit a dependence of rheological properties on equilibration time [4]. While it is unclear if all the above studies used appropriate protocols to anneal the samples *in-situ* in order to obtain results from equilibrated structures, their findings provide a useful starting point. A filament stretching rheometer with state-of-the-art temperature control allows for *in-situ* annealing prior to performing uniaxial extensional flow, with minimal experimental errors [13].

Investigation of ionomers in nonlinear shear is limited as well, in part, due to the experimental difficulties to overcome artifacts such as edge fracture [14]. Takahashi *et al.* [15] have systematically investigated the nonlinear stress relaxation in ethylene-co-methacrylic acid ionomers as a function of ion content. They found that the damping function $h(\gamma) = G(t,\gamma)/G(t)$, a measure of material's nonlinear response, was unaffected by ionic interactions at low ion content, whereas strong strain softening was reported at higher ion content. The implementation of the cone-partitioned plate (CPP) geometry on strain-controlled rheometers has opened the route for advancing the polymer melt rheology field by performing artifact-free nonlinear shear experiments [14,16].

Recently, single-ion conducting polymers, or ionomers, have found great interest as candidate materials in energy storage devices, such as lithium ion batteries [3,8,17,18]. Polymer electrolytes without volatile solvents as materials for battery applications are safer when compared to conventional liquid electrolytes. However, the ionic conductivity of these materials is still far below the 1 mS/cm target for practical applications [19]. This is attributed to its coupling with segmental chain dynamics [18,20]. Consequently, enhancing mechanical performance (elasticity and glass transition temperature T_g) often lowers conductivity, making it challenging to find the right balance. Poly(ethylene oxide) (PEO)-based ionomers have been studied quite extensively due to the superior cation solvation ability [3,8,17,18,21]. Recently, Chen *et al.* [3] have investigated linear viscoelastic properties of amorphous copolyester ionomers synthesized via condensation of sulfonated phthalates with mixtures of PEO and poly(tetramethylene glycol) (PTMO) [3]. This study is based on unentangled ionomer systems, where the rich linear viscoelastic (LVE) properties are attributed to the ionic clusters [8]. By introducing low T_g PTMO along the backbone of the PEO ionomer, the elasticity was remarkably improved due to stronger ionic clusters formed in the PTMO-rich domain.

This article is part of an ongoing investigation on viscoelastic properties of polyether-ester ionomers initiated by Colby and coworkers [8,18]. In this work, we examine nonlinear shear, and uniaxial extensional rheology of PTMO ionomer neutralized with Na (PTMO-Na) and PTMO ionomer neutralized with Li (PTMO-Li), one coionomer PEO25-PTMO75 neutralized with Na (PEO25-PTMO75-Na) and a coionomer PEO25-PTMO75-Li neutralized with Li. In the case of the coionomer, 25 mol. % of the diols are PEO, and 75 mol. % are diols of PTMO. The effect of PEO phase on shear and extensional melt behavior is elucidated by comparing the properties of PTMO-ionomer, and the PEO25-PTMO75-coionomer melts at similar flow conditions.

II. EXPERIMENTAL SECTION

A. Materials

Amorphous copolyester ionomers were synthesized via condensation of sulfonated phthalates with mixtures of poly(ethylene glycol) with $M = 600$ g/mol and PTMO with $M = 650$ g/mol [3]. The structures of PEO-PTMO-Na (Li) coionomers and PTMO-Na (Li) ionomers are shown in Fig. 1.

The LVE was remeasured and shown to be in good agreement with the published work [8] except for the LVE of the PTMO-Li ionomer, which is shifted to lower frequencies (by a factor of 4). This is likely due to the contamination of water. First, the Na ionomers were synthesized and then dialyzed extensively to replace Na with Li ion. For completely removing Na, more than ten times stoichiometric ions were chosen for each dialysis, and the process was repeated at least three times. This process has been standardized in Colby's lab so the remaining Na should be less than 0.1%. The water contamination is less controllable than the purity of ions based on our experience on these samples. Previous X-ray scattering results have shown that crystallization only occurs at low temperatures below 0 °C [18]; hence, our samples are amorphous at room temperature. In addition, at 20 °C, the copolymers microphase separates into PEO-rich and PTMO-rich domains with the majority of ions residing

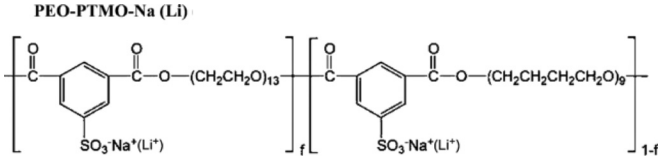

FIG. 1. Chemical structure of PEO-PTMO-Na (Li) coionomers with the fraction f of PEO spacer varied from 0.25 [PEO25-PTMO75-Na (Li)] to 0 [PTMO-Na (Li)].

TABLE I. Molecular weight M_n and T_g for the ionomers with Li and with Na counterions.

Sample	M_n (g/mol)	T_g (°C) Li	T_g (°C) Na
PEO25-PTMO75	6500	−48	−47
PTMO	6700	−63	−64

in the former [18] (see also Sec. III). The samples used in this work and their characteristics are given in Table I.

B. Moisture content

Recent studies on ionomers have shown that the presence of moisture can modify the rheological properties by lowering the viscosities and accelerating the terminal relaxation time [22,23]. Therefore, the samples were dried in a vacuum oven at 100 °C overnight prior to direct loading to the rheometer. Instrument quality Argon gas (Argon 99.999%, $O_2 < 2$ ppm, $N_2 < 5$ ppm, $H_2O < 3$ ppm) was used instead of air for releasing the vacuum inside the vacuum oven. This step minimizes oxidation of the sample. However, the samples oxidize over long residence times in the rheometer, making data reproducibility a major challenge. Overall, the samples investigated were very sensitive to humidity, temperature, and oxygen conditions. However, all reported data were obtained with the same protocol and were reproducible. To highlight the influence of moisture, we plot the linear viscoelastic master curve of PTMO-Li at $T_{ref} = 20$ °C in Fig. 2. The undried sample was left for one day at room temperature and atmospheric pressure. The impact of moisture on the rheological properties is striking. The moduli of the moist sample are decreased by more than one decade.

C. Uniaxial extensional rheology measurements

The extensional stress growth coefficient η_E^+ was measured as a function of time using filament stretch rheometers: DTU-FSR and VADER. Cylindrical stainless steel plates with a diameter of 5.4 mm were used for all measurements. Measurements were performed at constant Hencky strain rate imposed at the midfilament diameter using an online control scheme [24]. Samples were heated under nitrogen for 2 h at 100 °C prior to performing experiments. At such a temperature the ionomer flows easily and forms a nice axisymmetric shape when the top rheometer plate is brought into contact with the sample. All experiments were performed between 35 and 90 °C in a nitrogen controlled environment. The imposed stretch rates varied from 0.01 to 1 s^{-1}.

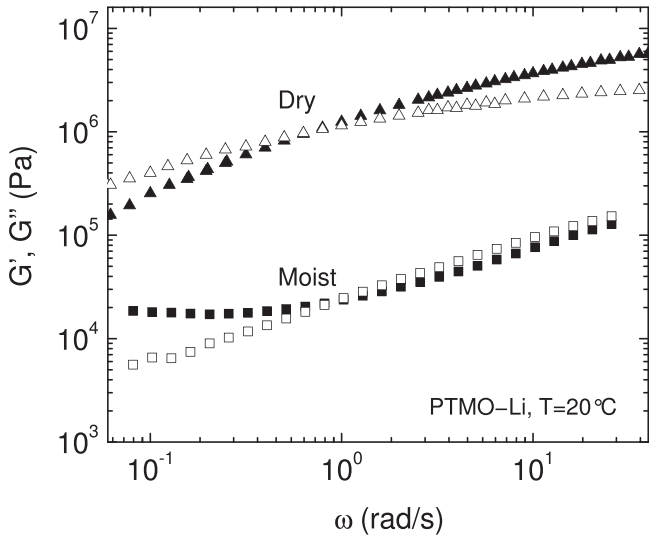

FIG. 2. LVE master curves of PTMO-Li at $T_{ref} = 20$ °C in dried and undried state (closed symbols G' and open symbols G'').

D. Nonlinear shear rheology measurements

Selected measurements were performed in nonlinear shear in order to compare the response of the ionomers (Table I) in such a weaker flow (due to rotational contribution as well) against those in uniaxial extension. The same sample treatment protocol was used in shear measurements as in extensional measurements. Shear rheology measurements were performed in a strain controlled rheometer (ARES 2kFRTN1, TA, USA) using a home-made stainless steel cone-partitioned-plate geometry with the following characteristics: measuring plate diameter 6 mm, cone angle 0.1 rad, the outer partition with an outer diameter of 20 mm and an inner diameter of 6.16 mm; thus, the gap between the partitions is around 80 μm. The plates were smooth (with several random scratches from use). In general, using grooved or cross-hatched plates in conjunction with cone or CPP geometry renders gap calibration problematic. Hence, we had to compromise and chose reasonably smooth plates. As a result, the issue of wall slip remains, and we discuss this below. For temperature control, the ARES convection oven with nitrogen flux was used, with a temperature control of ±0.1 °C [25].

Typically, a sample of diameter 6 mm and thickness 0.15 mm was placed in the rheometer and shaped at 100 °C. Dynamic frequency sweeps (with linear strain amplitude $\gamma_0 = 0.04$ and imposed frequency range $\omega = 0.1$–100 rad/s) were performed in order to check the linear rheological data for consistency over a broad range of temperatures (0–100 °C). Subsequently, start-up of steady shear was performed at 60 °C for PTMO-Na at constant values of shear rate ranging from $\dot{\gamma} = 0.02$ to $0.7 s^{-1}$. Using the time-temperature superposition frequency scale shift factor, the measurements at 60 °C were shifted to 80 °C. The maximum imposed deformation ($\dot{\gamma}t$) was limited to four strain units. Between consecutive tests, the material was rejuvenated at 100 °C for 15 min. It was found that this time was sufficient to thermally equilibrate the sample, as confirmed by subsequent linear rheological measurements. A similar procedure was utilized for the PEO25-PTMO75-Na coionomer for which the start-up of steady shear was performed at 45 °C at constant values of shear rate ranging from $\dot{\gamma} = 0.1$ to $1 s^{-1}$, with a maximum imposed deformation limited to 20 strain units. In general, the consistency of linear and nonlinear rheological data was confirmed by the use of the above protocols, the fact that the linear spectra were identical to those of Tudryn *et al.* [18] and the matching of the linear viscoelastic envelope to the nonlinear data at short times (e.g., Figs. 3 and 8).

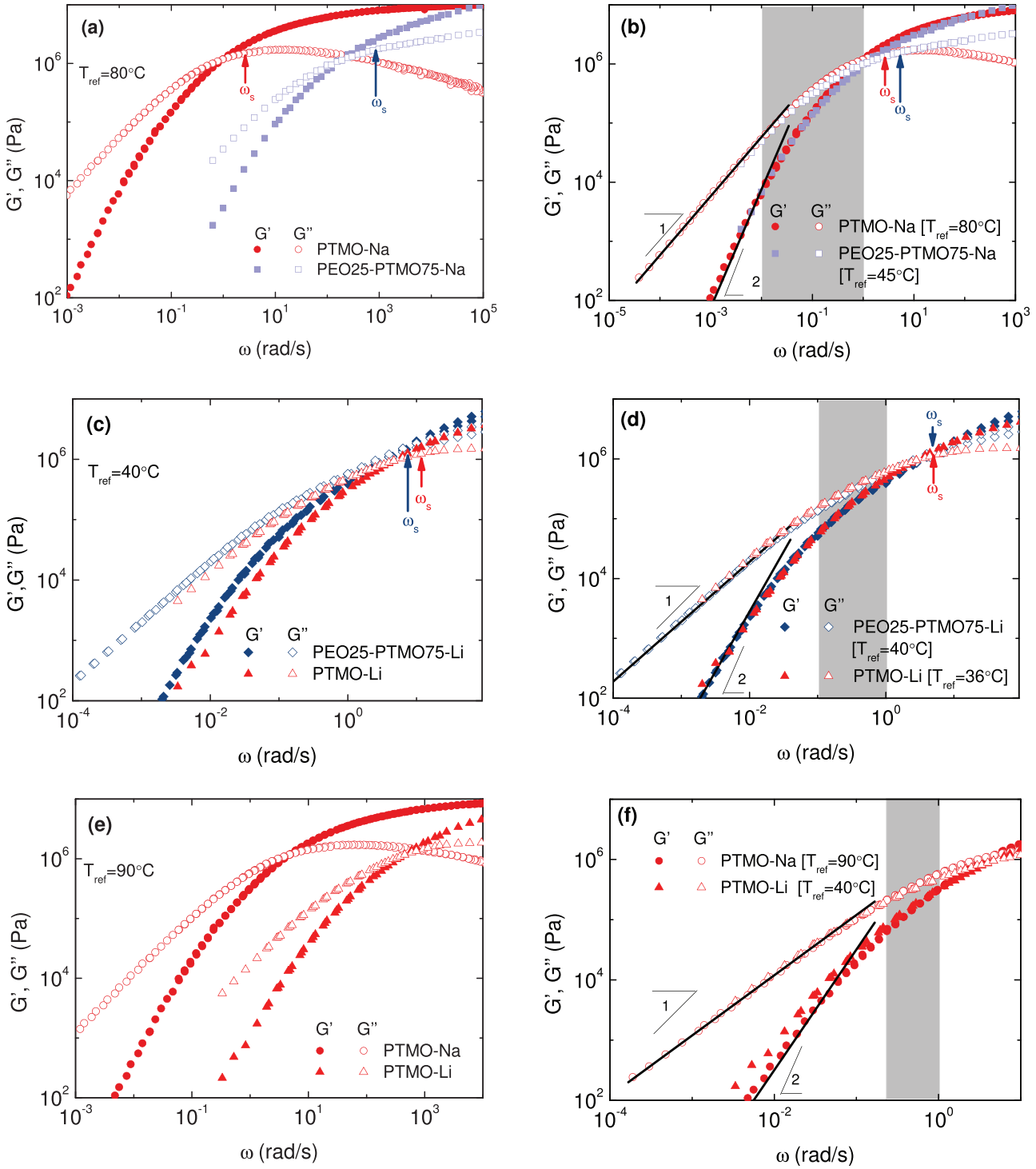

FIG. 3. LVE master curves of (a) PTMO-Na and PEO25-PTMO75-Na at $T_{ref} = 80\,^{\circ}\mathrm{C}$, (c) PTMO-Li and PEO25-PTMO75-Li at $T_{ref} = 40\,^{\circ}\mathrm{C}$, (e) PTMO-Na and PTMO-Li at $T_{ref} = 90\,^{\circ}\mathrm{C}$. The corresponding master curves on the right (b), (d), and (f) are compared at different T in order to have an overlapped terminal regime (see text). Plots (b), (d), and (f) correspond to conditions of identical Weissenberg number. The gray areas indicate the measured range of frequencies (respectively, Weissenberg numbers), see also Fig. 7(b) for PTMO-Na.

III. RESULTS AND DISCUSSION

A. Linear viscoelasticity

LVE results are shown in Figs. 3(a)–3(f), in order to highlight the regions investigated in nonlinear rheological measurements. Plots (a), (c), and (e) represent the actual measured data, which are shifted to match the crossover frequencies in plots (b), (d), and (f), as described below. This provides the investigated regions with identical Weissenberg number, based on the crossover frequency, for each experimental pair of samples [see also Fig. 7(b)]. Note that this shifting contains information about the relative strength of bonds in the systems.

Figures 3(a) and 3(c), show the influence of addition of PEO phase with Na and Li as the counterion, respectively. Our simple approach consists of comparing the LVE master curves at different temperatures to have an overlapped

terminal flow regime. The effect of PEO phase can then be elucidated under a range of applied strain rates both in extension and nonlinear shear. Figure 3(e), shows the ion dependence of LVE for the PTMO ionomers. For investigating the influence of ion on the physical mechanism of strain hardening in extensional flow, LVE master curves for PTMO-Li and PTMO-Na are shifted as shown in Fig. 3(f). Same applies to Figs. 3(b) and 3(d). For unentangled ionomers, the terminal relaxation time τ depends on the temporary ionic associations. The ionic groups attached to the chain, hop between aggregates with a characteristic time $\tau_s = 1/\omega_s$, also called the lifetime of ionic associations. The higher the association lifetime, the longer is the terminal relaxation time. Polydispersity in molecular weight results in broadening of the lower crossover frequency region because of the distribution in the number of polymer modes, each associated with a contribution to the moduli [26]. The ionomers used in this study are polydisperse (*polydispersity* ≈2.0) and exhibit terminal slopes of $G''(\omega)$, and $G'(\omega)$ (represented in black solid lines). The terminal relaxation time can be evaluated as

$$\tau = \lim_{\omega \to 0} \left[\frac{G'}{\omega G''} \right]. \tag{1}$$

The association lifetime can, thus, be obtained as

$$\tau_s = \frac{\tau}{N_s^2}, \tag{2}$$

where $N_s = 7$ [3,8] is the number of sticky Rouse segments per chain, which is the same for PTMO and PEO25-PTMO75 because the M_n and the spacer molecular weights are nearly identical (see Table I). $\tau_s = 1/\omega_s$ is indicated by arrows in Fig. 3.

B. Uniaxial extensional rheology

1. Effect of PEO with Na counterion

We now examine the extensional rheology in the context of the LVE data presented earlier. Figures 4(a) and 4(b) show the stress growth coefficients η_E^+, as a function of time for the PTMO-Na ionomer and the PEO25-PTMO75-Na coionomer at various strain rates $0.01\,\mathrm{s}^{-1} \leqslant \dot{\epsilon} \leqslant 1\,\mathrm{s}^{-1}$. The strain rates are always increasing from right to left. The LVE envelope obtained using a multimode Maxwell fit from LVE oscillatory shear data is plotted as a solid line. The extensional data are consistent with the predictions of linear viscoelasticity at short extension times. All the samples, fracture

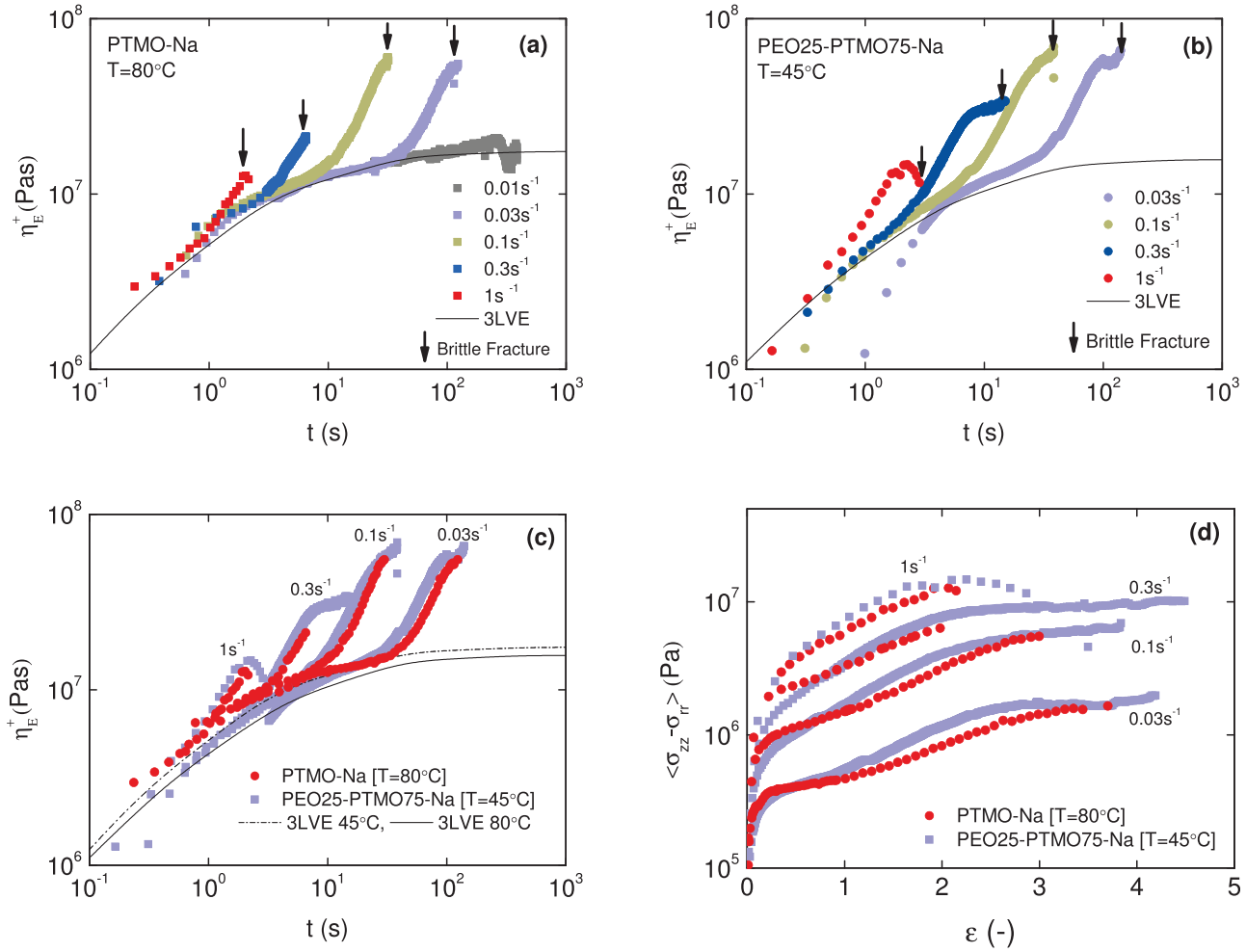

FIG. 4. Top: Extensional stress growth coefficients at different Hencky rates as a function of time for (a) PTMO-Na at 80 °C, and (b) PEO25-PTMO75-Na at 45 °C, chosen because these temperatures have nearly identical LVE [see Fig. 3(b)]. Bottom: (c) comparison of stress growth coefficient as a function of time for PTMO-Na at 80 °C: and PEO25-PTMO75-Na at 45 °C, (d) same data as in Fig. 4(c) plotted as true extensional stress versus Hencky strain. Black arrows highlight the end of this experiment due to brittle fracture of the filament into two halves. Lines are the linear viscoelastic envelopes.

into two halves in a brittle fashion. The black arrows in Figs. 4(a) and 4(b) indicate fracture of the filament. Detailed study of brittle fracture of ionomers is discussed elsewhere [27].

At very low strain rates ($<0.03\,s^{-1}$) the stress growth coefficient follows the LVE envelope attaining steady state at large Hencky strains. However, at higher strain rates, a departure above the LVE envelope (often termed strain hardening) is noticed. The pattern of strain hardening observed here, i.e., decreasing strain hardening with increasing strain rate, resembles that of long-chain lightly branched polymers such as metallocene-based linear low-density polyethylenes (LCB-mLLDPE) [28]. Highly branched low-density polyethylenes exhibit opposite behavior. The extension rates probed in Figs. 4(a) and 4(b) are smaller than the inverse of the association lifetime [indicated in Fig. 3(b)], leading to an effective Weissenberg number below 1 (see also Fig. 7). Note that similar trend of decreasing strain hardening with increasing strain rate was observed for entangled PBd-based telechelic ionomers bearing carboxylate groups neutralized with Rb, PBd-COORb, but not for PBd-COOLi (in that case increasing hardening with decreasing rate was observed) or PBd-COONa and PBb-COOK (no hardening observed) [11]. With telechelic polymers, the spatial organization is expected to be very different from the present sulfonated systems, restricting the comparison to the qualitative level. These data were obtained at strain rates spanning a range from below to above the terminal crossover frequency. Further, sulfonated oligostyrene polystyrenes neutralized with Rd exhibited strain hardening that depended on the Weissenberg number (based on the terminal crossover frequency). Although it is not possible to extract unambiguous conclusions due to the limited data and some issues at short times (poor comparison with LVE line), it appears that for Weissenberg numbers well above 1, strain hardening decreased with increasing extension rate, whereas for lower values, even below 1, it increased with increasing extension rate [12]. One may conclude from this comparison that the interplay of bonding interactions (with varying strength and bond distribution, often leading to cluster formation [4]) with chain dynamics and flow rate dictates the response of ionomers in nonlinear deformations. However, the available data are insufficient to draw more concrete conclusions. Additional systematic rheological and structural evidence will be necessary in order to further elucidate the role of these parameters on the macroscopic properties of ionomers. In particular, we believe that our approach of using the same Weissenberg number is the way forward for comparing nonlinear data.

In order to elucidate the effect of addition of 25% PEO with Na counterion, a comparison between PTMO-Na and PEO25-PTMO75-Na is shown in Fig. 4(c). Although PEO25-PTMO75-Na is chemically different than PTMO-Na, identical strain hardening is observed with and without PEO because the slowest associations in the coionomer are in the PTMO-rich phase. The plot of true extensional stress as a function of Hencky strain in Fig. 4(d) indicates that incorporation of 25% PEO to the PTMO-ionomer increases the maximum Hencky strain at fracture. Although for strain rates smaller than $1\,s^{-1}$, it appears that η_E^+ reaches a constant value, it does not represent a true steady state because the material fractures at the end of each experiment. Such a behavior is different from classical linear polymer melts, where a steady state in η_E^+ is achieved at large Hencky strains followed by thinning of the filament rather than fracture [29].

2. Effect of PEO with Li counterion

We now investigate the effect of PEO with Li as the counterion within the context of the LVE presented in Figs. 3(c) and 3(d). With Li as the counterion, the activation energy for ionic hopping is smaller than with Na counterion [3]. Figures 5(a) and 5(b) compare PTMO-Li and PEO25-PTMO75-Li in extensional deformation. In Fig. 5(b), the material stretches more with the addition of PEO25% to the PTMO-Li ionomer. We conclude that addition of high solvating PEO makes the material significantly more ductile.

In our previous study, X-ray scattering revealed strong nanophase separation for PEO and PTMO in the coionomers [18]. Fourier transform infrared spectroscopy (FTIR) revealed the different aggregation status of the ions within the system. A combination of these two results suggests that

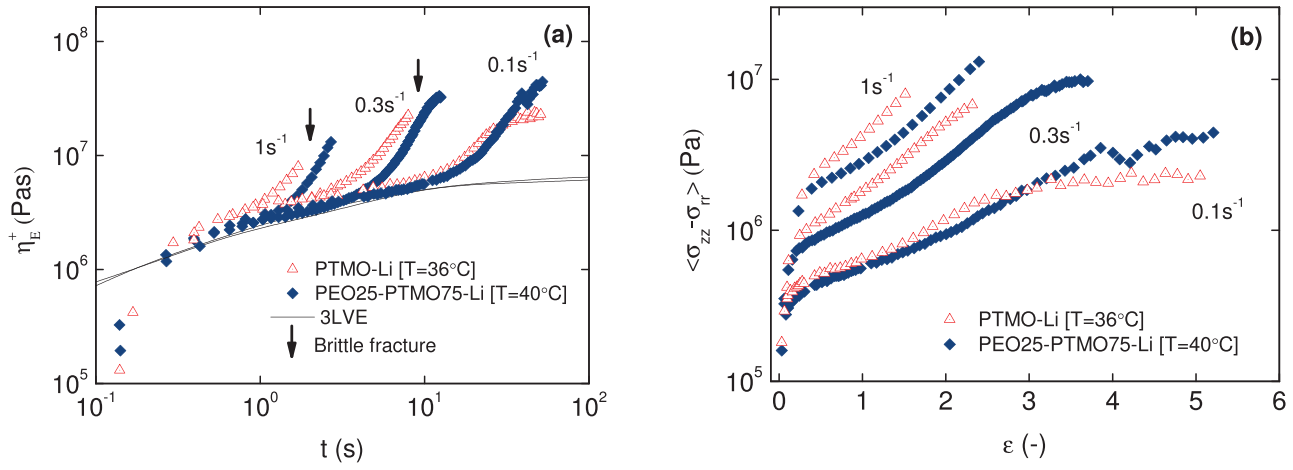

FIG. 5. (a) Comparison of extensional stress growth coefficient as a function of time for PTMO-Li and PEO25-PTMO75-Li, (b) same data plotted as true extensional stress versus Hencky strain. Lines are the LVE envelopes.

the ionic groups can be classified into three groups: Taking a number fraction of PEO block as f, the ionic groups having both sides connected to the PEO spacers with fraction f^2 are located in the PEO phase. Similarly, a fraction of the $(1-f)^2$ ionic groups is located in the PTMO phase, leaving a fraction $1-f^2-(1-f)^2=2f(1-f)$ ions at the PEO/PTMO interface. The higher ductility after incorporating the PEO block should be related to the nonuniform ionic dissociation times for the ionic groups of the coionomers. For the PEO25-PTMO75-Na and -Li, the fraction of ions within the PEO, PTMO domains, and at the interface are 56%, 6%, and 38%, respectively [3]. The ionic groups within the PEO phase keep more weakly associated than those in the PTMO phase. For example, the lifetime of ionic groups was estimated from LVE to be $\tau_s=4\,\mu$s for PEO-Na at $T_{ref}=45\,^\circ$C and $200\,\mu$s for PEO-Li at $T_{ref}=40\,^\circ$C, which is much shorter than τ_s estimated for the sample as a whole shown earlier in Fig. 3, which should be mainly controlled by those ionic groups that are strongly aggregated in the PTMO domains. The ionic groups at the interface should have lifetime in between those in PEO and PTMO domains. Therefore, for the PEO25-PTMO75-Na and -Li, τ_s mentioned in Eq. (2) is an empirical average association lifetime for all the ionic associations, namely, the ionic associations within the PEO, PTMO domains, and those at the interface. For the coionomer subjected to an elongation rate or shear rate less than $1\,s^{-1}$ at T_{ref} (Fig. 5), the ionic groups within the PEO phase and at the interface should be able to move freely to adjust the conformation of a chain distributed around the PEO and PTMO microdomains, which should be responsible to the extra ductility seen for the PEO25/PTMO75-Na and Li at T_{ref}.

3. Effect of counterion (Na and Li)

For investigating the ion dependence of strain hardening [see the respective LVE in Figs. 3(e) and 3(f)], a comparison of PTMO-Na and PTMO-Li is presented in Fig. 6. The observed identical strain hardening response is due to the same Weissenberg number being used [Fig. 2(f)]. This confirms our earlier statement about the shifting of plots in Fig. 2(e), which reflects different bonding strength of sulfonate groups in PTMO-Na and PTMO-Li, as expected [30]. However, differences were reported for PBd-COONa and PBd-COOLi telechelics [11] at different Weissenberg numbers.

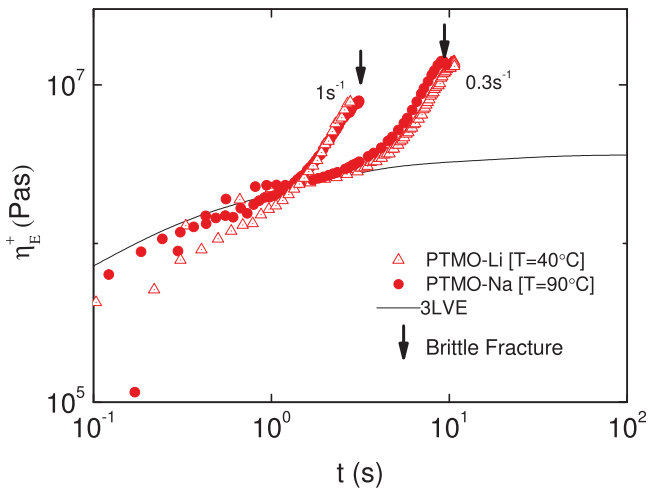

FIG. 6. Comparison of extensional stress growth coefficient at two different Hencky rates as a function of time for PTMO-Na at 90 °C, and PTMO-Li at 40 °C.

4. Extensional deformation of PTMO-Na ionomer: From melt to a "neo-Hookean" solid

We now turn our focus on the PTMO-Na ionomer. Figure 7(a) summarizes the results from extensional rheology measurements performed at $T=40$, 60, 80, and 90 °C. For testing the validity of time-temperature-superposition for ionomers in nonlinear extensional flows, a master plot is shown in Fig. 7(b) at $T_{ref}=80\,^\circ$C. The stress growth coefficient and time have been reduced by the respective temperature dependent shift factors, a_T. The shift factors for $T=40$, 60, and 90 °C are 0.0017, 0.03, and 4.21, respectively. As mentioned earlier, in order to quantify the degree of nonlinearity, we use the Weissenberg number based on the sticker lifetime $Wi=\dot{\epsilon}\tau_s$. Two regimes are noticeable: for $Wi<1$ filaments undergo strain hardening before eventually breaking in a brittle fashion (shown in top right region); on the other hand, for $Wi>1$, no strain hardening is observed (shown in bottom left region). In fact, the filaments fracture right on top of the LVE envelope. This behavior is *opposite* to that of entangled linear polymer melts far above T_g, where strain hardening always increases with increasing strain rates [31,32]. The inset plot shows the LVE of PTMO-Na ionomer in order to provide a guide for the corresponding regions probed.

The strain rate dependence of true extensional stress as a function of Hencky strain is shown in Fig. 7(c). The black solid line indicates the neo-Hookean [33] stress prediction based on the plateau modulus G_N^0 of PTMO-Na given by

$$\sigma_{zz}-\sigma_{rr}=G_N^0(\lambda^2-\lambda^{-1}). \tag{3}$$

Here, σ_{zz} and σ_{rr} are the axial and radial components of stress, respectively, and stretch ratio $\lambda=\exp\dot{\epsilon}t$. The neo-Hookean model does not take into account the finite extensibility of polymer chains made up of N segments [33]. The neo-Hookean stress corresponds to affinely deforming a permanently cross-linked network, and hence, represents an upper limit because it does not account for the dissipative mechanisms during nonlinear deformation. In all cases, the experimental stress values are below those predicted from the neo-Hookean model. For $Wi>1$, small Hencky strain values are achieved, and the true extensional stress at fracture is close to the neo-Hookean stress prediction. On the other hand, for $Wi<1$, the difference between true extensional stress at break and the model increases, while the material is able to stretch to higher Hencky strain values. The emerging picture is that of a transition from a hard-brittle to soft-ductile state. In the hard-brittle state, the material exhibits a nearly strain-rate independent response [see Figs. 7(b) and 7(c) for $Wi>1$]. This finding suggests that although these materials are elastic for $Wi>1$, their response in extension is brittle when stretched faster than their crosslink lifetime. Conventional polymer melts can be

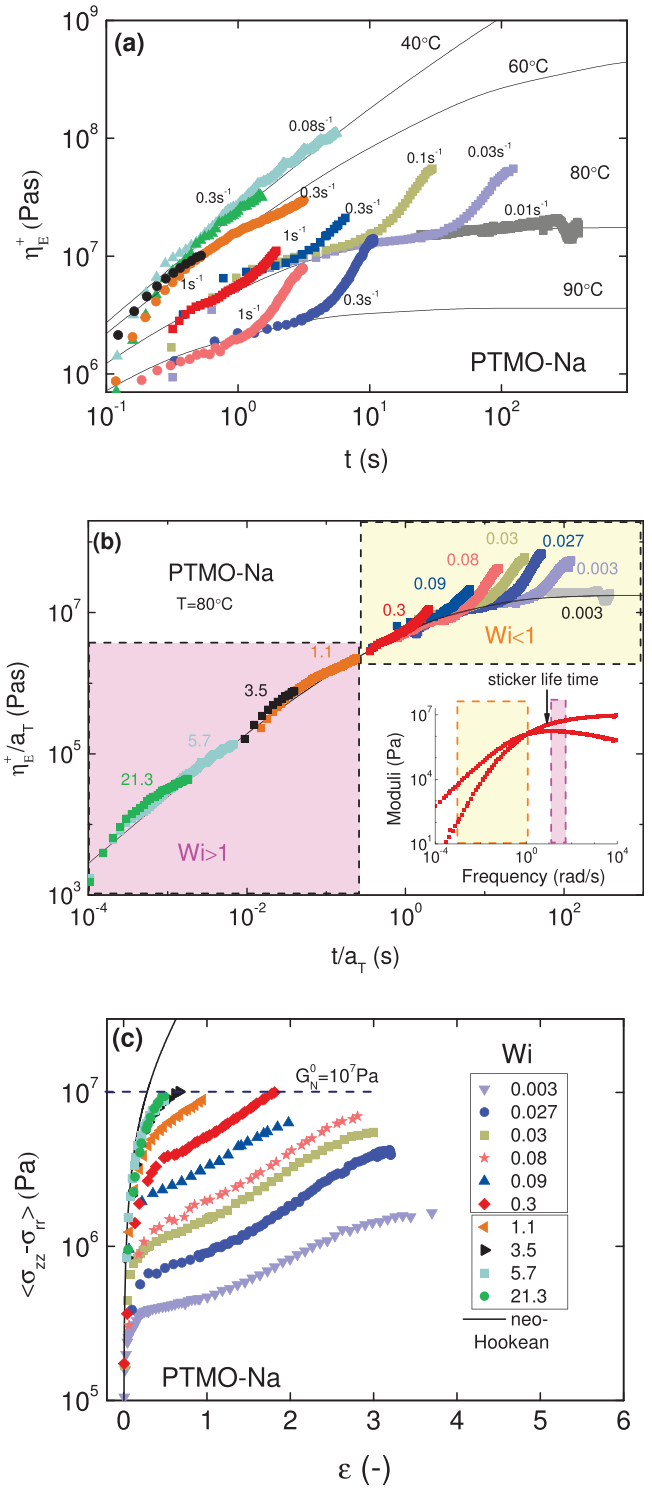

FIG. 7. (a) Extensional stress growth coefficient as a function of time at four temperatures, 40, 60, 80, and 90 °C for PTMO-Na, (b) master plot of extensional rheology at $T_{ref} = 80$ °C with numbers indicating Wi and the inset depicts LVE in order to provide a guideline for the corresponding regions probed, (c) true extensional stress versus Hencky strain for different rates and temperatures, corresponding to (a). The thin black line is the neo-Hookean stress prediction, which is the stress level, where the high rate ($Wi > 1$) samples break.

stretched to extensional stress levels much higher compared to the plateau modulus. For example, the maximum stresses reached with highly entangled polystyrene are about $40G_N^0$ [29,31,32]. However, maximum stress values that can be achieved with the PTMO-Na ionomer is in the order of $G_N^0 (\approx 10^7)$ Pa [see dashed line in Fig. 7(c)]. This result highlights the difference in the nature of the physical interactions in ionomers compared to the entanglements in classical polymers.

C. Nonlinear shear rheology

Figure 8(a), depicts the time evolution of shear stress at different shear rates for PTMO-Na, in the form of shear stress versus shear strain ($\gamma = \dot{\gamma} t$). Note that the range of strains covered is small for PTMO-Na, with the maximum strain being 4 u (here we show data up to strain = 3 for clarity). The transient data at small strains (or short times) collapse onto the LVE envelope as shown in the shear stress growth coefficient of Fig. 9. Furthermore, the same qualitative behavior is observed for a wide range of applied shear rates (for 0.6–20 s^{-1}). In particular, the stress reaches a peak value (at the LVE envelope as seen in Fig. 9) and then drops dramatically (by as much as one decade) before reaching steady state. More importantly, for $Wi > 1$ the stress reaches almost the same steady state value, independent of shear rate and drops stepwise, pointing to heterogeneous flow response. In fact, this strongly suggests the presence of instabilities, and in particular, wall slip and/or shear banding. Given the high plateau modulus of this material (exceeding 10^7 Pa) we tentatively interpret this behavior as slip. Indeed, it is known that polymers with modulus of 10^6 Pa (such as PBd) or higher are prone to wall slip [34]. Therefore, the polymer can barely respond to shear and even at strains of just over 0.2 u, it appears that it detaches from the plate of the rheometer (at least partly). This behavior is in contrast to the response of the same material in uniaxial extension (Fig. 4), where, in the absence of shear the material can deform but will eventually fracture at Hencky strains below 5 (see also Fig. 9). Hence, our conclusion is that this brittle material cannot be sheared and the erratic behavior of Fig. 8(a) is due to wall slip instabilities.

Remarkably, when we introduce 25% of PEO comonomer into the ionomer, the schematics shown in Fig. 8(a) alters substantially. This is shown in Fig. 8(b), where the transient shear stress is plotted against the accumulated strain. We note that much larger strains (by almost 2 decades) are achieved compared to pure PTMO-Na. More importantly, whereas at low strains (or early times up to about 0.3 s) the transient stress data follow the LVE envelope, for higher strain we observe an overshoot, which becomes more evident as the shear rate increases. After the overshoot, the stress approaches a steady state for 0.1 and 0.3 s^{-1}, but this is not the case for the two higher shear rates, for which the data suggest the influence of edge fracture since the stress keeps on decreasing without the evidence of the steady state being approached [14]. It is interesting to observe further that the stress overshoot occurs at strains between 2 and 3 for all rates; here, it is tempting to recall that entangled linear flexible polymers exhibit a peak strain value of about 2.3 at low rates due to orientation (the Doi–Edwards prediction), which increases eventually with shear rate due to stretching. Finally, the shear data corroborate the conclusions from the

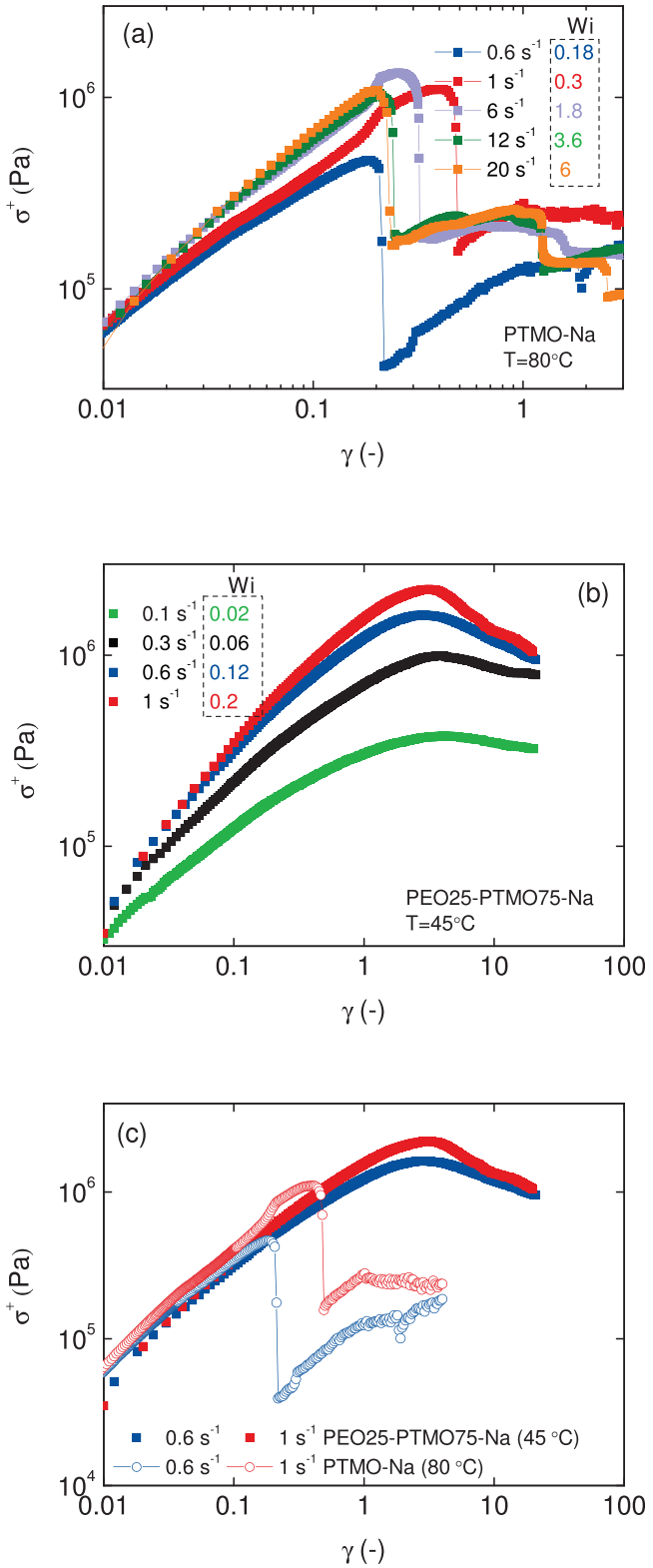

FIG. 8. Transient nonlinear shear data at different shear rates for (a) PTMO-Na at $T = 80\,^{\circ}\mathrm{C}$, (b) PEO25-PTMO75-Na at $T = 45\,^{\circ}\mathrm{C}$, (c) comparison of transient shear stress versus shear strain for PTMO-Na at $T = 80\,^{\circ}\mathrm{C}$ and PEO25-PTMO75-Na at $T = 45\,^{\circ}\mathrm{C}$, where the temperatures were chosen so as to match LVE [see Fig. 3(b)].

extensional data of Fig. 4, where the same materials can deform (and eventually fracture) at higher Hencky strain compared to brittle PTMO-Na. Therefore, the overall picture is substantially different from that of Fig. 8(b). Clearly, the

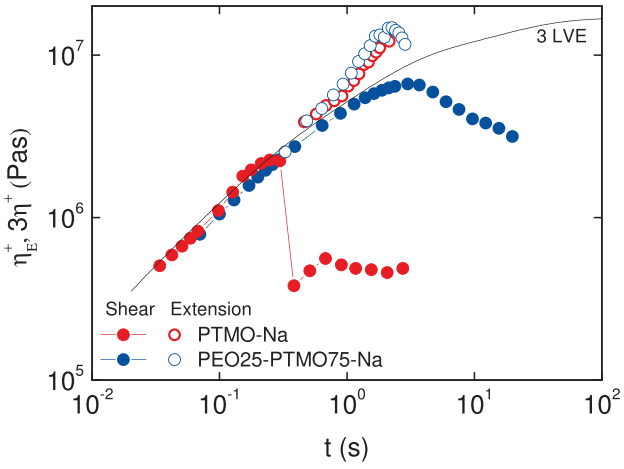

FIG. 9. Comparison of PTMO-Na ionomer ($T = 80\,^{\circ}\mathrm{C}$) with the PEO25-PTMO75-Na copolymer ionomer ($T = 45\,^{\circ}\mathrm{C}$) undergoing nonlinear shear and extension at a deformation rate fixed to $1\,\mathrm{s}^{-1}$. Open symbols represent extensional data showing strain hardening prior to brittle fracture, whereas filled symbols represent nonlinear shear data.

incorporation of ductile PEO makes the copolymer shear-processable. The latter can be appreciated in the comparative plot of Fig. 8(c).

D. Comparison of nonlinear shear and extensional rheology

We now compare the nonlinear rheological response of the PTMO-Na ionomer and the PEO25-PTMO75-Na coionomer under nonlinear shear and extensional deformations at identical conditions. This is shown in Fig. 9, where the transient extensional stress growth coefficient and three times the shear stress growth coefficient are depicted as functions of time, along with the LVE envelope. The deformation rate is fixed to $1\,\mathrm{s}^{-1}$ and the temperature for PTMO-Na is $80\,^{\circ}\mathrm{C}$, while the temperature for PEO25-PTMO75-Na is $45\,^{\circ}\mathrm{C}$ [see also Fig. 3(b)]. Transient shear stress growth coefficient data (shown by closed symbols) are vertically shifted by a factor of 3 (Trouton ratio). In nonlinear shear flow, the PEO25-PTMO75-Na coionomer deforms up to the overshoot (at a strain of about 2.5, which can be considered as a yield strain), whereas the respective strain at which wall slip commences for PTMO-Na is about 0.3. We also observe the already discussed big difference in shear and extension for PTMO-Na. Whereas the brittle PTMO-Na ionomer cannot be sheared beyond $\gamma \cong 0.3$ and responds erratically, it deforms in extension, albeit weakly, and fractures at $\epsilon \cong 2$. The ductile PEO25-PTMO75-Na coionomer deforms uniformly to much larger strains in both shear and extension. Eventually, it fractures in extension at $\epsilon \cong 2.8$ and yields in shear at $\gamma \cong 2.5$ (subsequently being affected by edge fracture).

IV. CONCLUSIONS

In this study, the nonlinear shear and uniaxial extensional rheology of polyether-ester-sulfonate ionomers were investigated. The ionomers showed strain hardening at extension

rates below the reciprocal of the sticker lifetime τ_s. The magnitude of strain hardening *decreased* as the Hencky strain rates approached $1/\tau_s$. Since the ionomers used in this study are unentangled, the strain hardening is attributed to the physical crosslinks, which comprise ionic clusters. Despite significant elasticity of these ionomers, they fractured in a brittle fashion in extension. The high-plateau modulus PTMO-Na exhibits a response akin to a brittle material: it fractures at low Hencky strains in extension and cannot be sheared homogeneously due to instabilities (predominantly wall slip). The effect of counterion on the extensional rheological response was also investigated by comparing PTMO-Na and PTMO-Li. Identical strain hardening and fracture were observed at the same Weissenberg number. Further, the effects of 25% PEO addition on the extensional rheological properties were studied. Clearly, the coionomer is more ductile, as confirmed by its ability to deform more under both shear and extension. However, even the more ductile coionomer shows limits for how much it can deform. In uniaxial extension, it always exhibits tensile fracture, while in shear flows it exhibits edge fracture at $\gamma \cong 2.5$. Results indicate that incorporating PEO comonomer into the PTMO-Na/Li ionomer increases the toughness of the material by increasing the maximum strain both in shear and extension.

The overall difference in nonlinear deformation and fracture between bulk PTMO and its PEO-based coionomer is attributed to the presence of PEO, which makes the system more ductile. Since the PEO-rich domains offer better ion conduction, the coionomer has a better compromise between mechanical performance subject to large deformation and ion conduction.

ACKNOWLEDGMENTS

The work leading to these results has received funding from the People Programme (Marie Curie Actions) of the European Union's Seventh Framework Programme (FP7/2007-2013), SUPOLEN under REA Grant Agreement No. 607937, and the Aage and Johanne Louis-Hansen foundation. Q.C. and R.H.C. thank the National Science Foundation for support from DMR-1404586.

References

[1] Tierney, N. K., and R. A. Register, "Ion hopping in ethylene - methacrylic acid ionomer melts as probed by rheometry and cation diffusion measurements," Macromolecules **35**, 2358–2364 (2002).

[2] Eisenberg, A., and F. E. Bailey, *Coulombic Interactions in Macromolecular Systems* (American Chemical Society, Washington, DC, 1986).

[3] Chen, Q., H. Masser, H.-S. Shiau, S. Liang, J. Runt, P. C. Painter, and R. H. Colby, "Linear viscoelasticity and Fourier transform infrared spectroscopy of polyether-ester-sulfonate copolymer ionomers," Macromolecules **47**, 3635–3644 (2014).

[4] Stadler, F. J., W. Pyckhout-Hintzen, J.-M. Schumers, C.-A. Fustin, J.-F. Gohy, and C. Bailly, "Linear viscoelastic rheology of moderately entangled telechelic polybutadiene temporary networks," Macromolecules **42**, 6181–6192 (2009).

[5] Weiss, R. A., and W.-C. Yu, "Viscoelastic behavior of very lightly sulfonated polystyrene ionomers," Macromolecules **40**, 3640–3643 (2007).

[6] Weiss, R. A., and H. Zhao, "Rheological behavior of oligomeric ionomers," J. Rheol. **53**, 191–213 (2009).

[7] Vanhoorne, P., and R. A. Register, "Low-shear melt rheology of partially-neutralized ethylene - methacrylic acid ionomers," Macromolecules **29**, 598–604 (1996).

[8] Chen, Q., G. J. Tudryn, and R. H. Colby, "Ionomer dynamics and the sticky Rouse model," J. Rheol. **57**, 1441–1462 (2013).

[9] Connelly, R. W., R. C. McConkey, J. M. Noonan, and G. H. Pearson, "Melt rheology of ion-containing polymers. I. Effect of ionic content in a model polyesterionomer," J. Polym. Sci. Part B: Polym. Phys. **20**, 259–268 (1982).

[10] Takahashi, T., J. Watanabe, K. Minagawa, and K. Koyama, "Effect of ionic interaction on elongational viscosity of ethylene-based ionomer melts," Polymer **35**, 5722–5728 (1994).

[11] Stadler, F. J., T. Still, G. Fytas, and C. Bailly, "Elongational rheology and brillouin light scattering of entangled telechelic polybutadiene based temporary networks," Macromolecules **43**, 7771–7778 (2010).

[12] Ling, G. H., Y. Wang, and R. A. Weiss, "Linear viscoelastic and uniaxial extensional rheology of alkali metal neutralized sulfonated oligostyrene ionomer melts," Macromolecules **45**, 481–490 (2012).

[13] Bach, A., H. K. Rasmussen, and O. Hassager, "Extensional viscosity for polymer melts measured in the filament stretching rheometer," J. Rheol. **47**, 429–441 (2003).

[14] Snijkers, F., and D. Vlassopoulos, "Cone-partitioned-plate geometry for the ARES rheometer with temperature control," J. Rheol. **55**, 1167–1186 (2011).

[15] Takahashi, T., J. Watanabe, K. Minagawa, J.-I. Takimoto, K. Iwakura, and K. Koyama, "Effect of ionic interaction on linear and nonlinear viscoelastic properties of ethylene based ionomer melts," Rheol. Acta **34**, 163–171 (1995).

[16] Schweizer, T., "Comparing cone-partitioned plate and cone-standard plate shear rheometry of a polystyrene melt," J. Rheol. **47**, 1071–1085 (2003).

[17] Armand, M., M. Duclot, and P. Rigaud, "Polymer solid electrolytes: stability domain," Solid State Ion **4**, 429–430 (1981).

[18] Tudryn, G. J., M. V. O'Reilly, S. Dou, D. R. King, K. I. Winey, J. Runt, and R. H. Colby, "Molecular mobility and cation conduction in polyether-ester-sulfonate copolymer ionomers," Macromolecules **45**, 3962–3973 (2012).

[19] Wang, Y., F. Fan, A. L. Agapov, T. Saito, J. Yang, X. Yu, K. Hong, J. Mays, and A. P. Sokolov, "Examination of the fundamental relation between ionic transport and segmental relaxation in polymer electrolytes," Polymer **55**, 4067–4076 (2014).

[20] Wang, Y., A. L. Agapov, F. Fan, K. Hong, X. Yu, J. Mays, and A. P. Sokolov, "Decoupling of ionic transport from segmental relaxation in polymer electrolytes," Phys. Rev. Lett. **108**, 088303 (2012).

[21] Lin, K.-J., K. Li, and J. K. Maranas, "Differences between polymer/salt and single ion conductor solid polymer electrolytes," R. Soc. Chem. Adv. **3**, 1564–1571 (2013).

[22] Chassenieux, C., and R. Je, "Elongation of telechelic ionomers under shear: A rheological and rheo-optical study," Macromolecules **33**, 1796–1800 (2000).

[23] Nishioka, A., T. Koda, K. Miyata, G. Murasawa, and K. Koyama, "The effects of small contents of water on melt rheology for ethylene-methacrylic zinc ionomers," Polym. J. **40**, 350–353 (2008).

[24] Román Marín, J. M., J. K. B. Huusom, N. J. Alvarez, Q. Huang, H. K. Rasmussen, A. Bach, A. L. Skov, and O. Hassager, "A control scheme

for filament stretching rheometers with application to polymer melts," J. Non-Newtonian Fluid Mech. **194**, 14–22 (2013).

[25] Yan, Z.-C., S. Costanzo, Y. Jeong, T. Chang, and D. Vlassopoulos, "Linear and nonlinear shear rheology of a marginally entangled ring polymer," Macromolecules **49**, 1444–1453 (2016).

[26] Shabbir, A., I. Javakhishvili, S. Cerveny, S. Hvilsted, A. L. Skov, O. Hassager, and N. J. Alvarez, "Linear viscoelastic and dielectric relaxation response of unentangled UPy-based supramolecular networks," Macromolecules **49**, 3899–3910 (2016).

[27] Shabbir A., Q. Huang, Q. Chen, R. H. Colby, N. J. Alvarez, and O. Hassager, "Brittle fracture in associative polymers: the case of ionomer melts," Soft Matter **12**, 7606–7612 (2016).

[28] Gabriel, C., and H. Münstedt, "Strain hardening of various polyolefins in uniaxial elongational flow," J. Rheol. **47**, 619–630 (2003).

[29] Bach, A., K. Almdal, H. K. Rasmussen, and O. Hassager, "Elongational viscosity of narrow molar mass distribution polystyrene," Macromolecules **36**, 5174–5179 (2003).

[30] Zundel, G., *Hydration of Intermolecular Interaction* (Academic, New York, London, 1969).

[31] Huang, Q., N. Alvarez, A. Shabbir, and O. Hassager, "Multiple cracks propagate simultaneously in polymer liquids in tension," Phys. Rev. Lett. **117**, 087801 (2016).

[32] Huang, Q., and O. Hassager, "Polymer liquids fracture like solids," Soft Matter **13**, 3470–3474 (2017).

[33] Doi, M., *Introduction to Polymer Physics* (Oxford University, New York, 1996).

[34] Hatzikiriakos, S. G., "Slip mechanisms in complex fluid flows," Soft Matter **11**, 7851–7856 (2015).